Wood Sci Technol (2018) 52:29–43
https://doi.org/10.1007/s00226-017-0944-3

ORIGINAL

Coupled two-dimensional modeling of viscoelastic creep of wood

Sabina Huč[1,2] · **Staffan Svensson**[1]

Received: 18 November 2016 / Published online: 24 August 2017

Abstract Three coupled two-dimensional viscoelastic creep models for orthotropic material are analyzed. The models of different complexity are mathematically formulated and implemented in a finite element software. Required viscoelastic material parameters are determined by calibration procedure, where numerical results are compared against experimentally obtained viscoelastic strains caused by tensile or shear loading. Finally, a comparison method is used to evaluate the accuracy of strain predictions of each particular model. The analysis shows that all the models are able to accurately predict viscoelastic creep simultaneously in two perpendicular directions for various periods of time and wood species. Calculated numerical values of the viscoelastic material parameters suitable for the three models and wood species, i.e., Douglas fir (*Pseudotsuga menziesii*), Norway spruce (*Picea abies*), Japanese cypress (*Chamaecyparis obtusa*), and European beech (*Fagus sylvatica* L.), under constant tensile loading are also given.

Introduction

Long-term performance of wood is strongly affected by a process of creep. It is understood as an increment of strain over time due to applied constant or changing load in a constant or changing environment. Timber structures are usually exposed

Electronic supplementary material The online version of this article (doi:10.1007/s00226-017-0944-3) contains supplementary material, which is available to authorized users.

✉ Sabina Huč
sabina.huc@hb.se

[1] Faculty of Textiles, Engineering and Business, University of Borås, 501 90 Borås, Sweden

[2] Division of Applied Mechanics, Ångström Laboratory, Uppsala University, 751 21 Uppsala, Sweden

to all four combinations during their service life, making designing timber structures challenging, and when accounting for wood as natural, heterogeneous, and anisotropic material, the task becomes even more so. Therefore, significant research efforts to improve mathematical, empirical, and numerical expressions for describing time-dependent behavior of wood have been undertaken. For simplicity, wood sections far enough from the stem are considered as orthotropic material. Viscoelastic creep is a pure creep response solely inflicted by a load's magnitude and its duration. Even though pure creep for load-carrying wood in ordinary varying climate is small in magnitude when compared to, for example, mechano-sorptive creep (Toratti and Svensson 2000), its formulation is a fundamental basis for the description of wood behavior, impacted by all sorts of environment variation (Hanhijärvi 1995; Bonfield et al. 1996; Hunt and Gril 1996; Hanhijärvi and Hunt 1998; Dubois et al. 2005, 2012; Colmars et al. 2014; Reichel and Kaliske 2015b). Several series of experimental data on viscoelastic creep strains in different orthotropic directions of wood under constant tensile loading are reported in Schniewind and Barrett (1972), Hayashi et al. (1993), Taniguchi and Ando (2010), and Ożyhar et al. (2013). Experimental data of viscoelastic shear strains is reported in Schniewind and Barrett (1972). The researchers point out the importance and difficulties of isolating the viscoelastic creep from other types of excitations that influence long-term behavior of wood. Constant environmental conditions are, therefore, required during the experiments in order to eliminate possible additional strains. Schniewind and Barrett (1972) and Hayashi et al. (1993) support their experimental work by theoretical considerations on creep compliance components. Taniguchi and Ando (2010) study time dependence of Poisson's ratios based on their experimental results. Frandsen (2007) discusses the existence of Poisson's ratios in orthotropic creep models and mathematically proves that diagonal components of the creep compliance matrices cannot scale proportionally to the diagonal components of the elastic compliance matrix as a ratio. Additionally, he shows that the off-diagonal components scale disproportionally to the diagonal components of all creep compliance matrices introduced in an orthotropic model. These findings are quite revolutionary and not easy to establish since they are violated in several creep models, for example, in Fortino et al. (2009), and Hassani et al. (2015). The coupled formulation of creep by Frandsen (2007) accounts for the necessary requirements about the compliance matrix. Another approach, where the requirements of the creep compliance matrix symmetry are fulfilled with defining relative creep functions, is found in Ormarsson (1999) and Reichel and Kaliske (2015a). On the other hand, Ando et al. (2013) and Jiang et al. (2016) have experimentally obtained the asymmetric creep compliance matrix of wood. In the present paper, three constitutive creep models of different complexity based on Frandsen's (2007) coupled two-dimensional formulation of creep for orthotropic material are studied. The models are implemented in a finite element software where numerical solution of time-dependent strain state is obtained. Viscoelastic material parameters (from now on referred to as material parameters, unless otherwise stated) of the models are calibrated against series of experimental data of different wood species. Extensive analysis and calibration of the proposed coupled two-dimensional formulation of creep of wood (Frandsen 2007) is novel and presents an easy

and efficient way of determining the characteristic material parameters for each wood species, i.e., Douglas fir (*Pseudotsuga menziesii*), Norway spruce (*Picea abies*), Japanese cypress (*Chamaecyparis obtusa*), and European beech (*Fagus sylvatica* L.).

Methods and modeling

Three coupled two-dimensional orthotropic constitutive models for viscoelastic creep of wood are studied. The studied creep models account for all the requirements about the symmetry and disproportionality of creep compliance matrices explained by Frandsen (2007). The models are composed of spring and dashpot elements, widely used for describing long-term viscoelastic behavior of a material. Spring represents linear elastic behavior, and the dashpot describes viscous behavior of the material that can be linear or nonlinear. In cases where the viscoelastic behavior of material under constant load level is modeled, a linear formulation of the dashpot is sufficient, since a nonlinear formulation will for this case still render linear behavior of the dashpot (Engelund and Svensson 2011; Caulfield 1985). Simple rheological model, Kelvin–Voigt (Flügge 1967) or simply Kelvin element, can be derived by a combination of the spring and the dashpot in parallel. More complex rheological models are assembled from different combinations of the basic elastic and viscous elements. Three types of assemblies for describing viscoelastic behavior of wood are used in this paper. They are schematically presented in Fig. 1. The same rheological assembly is considered in longitudinal and transverse direction of each model. Since the viscoelastic behavior is modeled by three different assemblies, namely Kelvin element, Kelvin element, and dashpot in series, and two Kelvin elements in series, the models are designated as K, KD, and KK model, respectively. Figure 2 illustrates the K model, while the same illustrative consideration can be applied to forming the KD and KK models with the proper assemblies included. Spring stiffnesses are designated by Q and dashpot viscosities by η. In Fig. 2, coupling of the longitudinal and transverse directions is graphically illustrated as a diamond geometry containing the rheological assembly. Since it is positioned in parallel, it enables response in

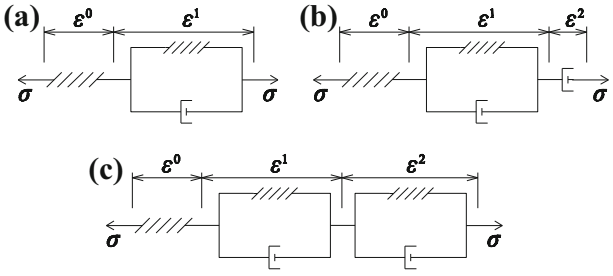

Fig. 1 Schematic illustration of rheological assemblies associated with the three orthotropic viscoelastic models, namely **a** K, **b** KD, and **c** KK model. σ denotes applied stress, ε^0 elastic strain, and ε^1 and ε^2 viscoelastic strains of dashpot or Kelvin elements

transverse direction when the longitudinal excitation is applied (Fig. 2a), and vice versa (Fig. 2b). Obviously, the direction of excitation and the transverse response are opposite in signs.

The total strains in longitudinal (L) and transverse directions (T), ε_{L} and ε_{T}, respectively, and the total shear strain (γ) are formed from a sum of elastic and viscoelastic parts

$$\begin{bmatrix} \varepsilon_{\mathrm{L}} \\ \varepsilon_{\mathrm{T}} \\ \gamma \end{bmatrix} = \sum_{i=0}^{2} \begin{bmatrix} \varepsilon_{\mathrm{L}}^{i} \\ \varepsilon_{\mathrm{T}}^{i} \\ \gamma^{i} \end{bmatrix} \tag{1}$$

where the elastic part is represented by $i = 0$ and the viscoelastic part by $i = 1$ for model K and $i = 1, 2$ for models KD and KK. In the rheological models (K, KD, and KK), it is assumed that viscoelastic strains are induced by the equilibrating stresses σ_{LL} and σ_{TL} for loading in L direction, and σ_{TT} and σ_{LT} for transverse loading.

$$\begin{bmatrix} \sigma_{\mathrm{L}} \\ \sigma_{\mathrm{T}} \end{bmatrix} = \begin{bmatrix} \sigma_{\mathrm{LL}} \\ \sigma_{\mathrm{TT}} \end{bmatrix} + \begin{bmatrix} \sigma_{\mathrm{LT}} \\ \sigma_{\mathrm{TL}} \end{bmatrix} \tag{2}$$

By considering the K model as illustrated in Fig. 2, for longitudinal loading, σ_{LL} and σ_{LT} equilibrate the stress in the spring and the stress in Kelvin element for longitudinal and transverse strains, respectively. Furthermore, in KD model, σ_{LL} and σ_{LT} equilibrate the stress in the spring, Kelvin element, and the dashpot for longitudinal and transverse strains, respectively. Similar consideration is applied for a transverse loading and KK model. Reader should be aware that σ_{LL}, σ_{LT}, σ_{TT}, and σ_{TL} do not have any physical meaning and are introduced due to derivation of the rheological models. Comprehensive description and derivation can be found in Frandsen (2007). The three rheological models are implemented in a commercial

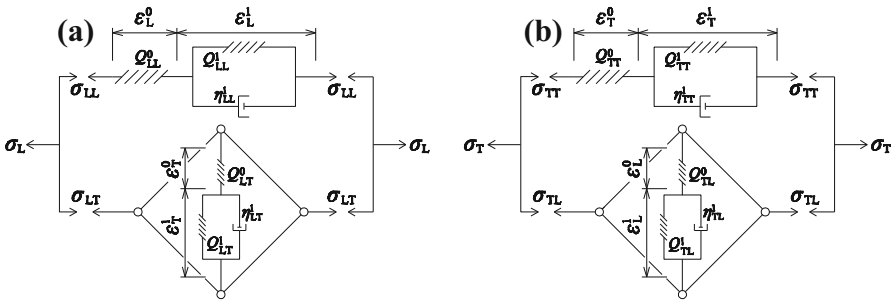

Fig. 2 Schematic representation of the two-dimensional orthotropic creep model for wood (K model) for **a** stress applied in longitudinal direction, σ_{L}, and **b** stress applied in transverse direction, σ_{T}. L designates longitudinal direction, T transverse direction, and LT and TL the coupling between L and T directions. Spring stiffnesses are designated by Q and dashpot viscosities by η. ε^0 is elastic strain, and ε^1 viscoelastic strain. σ_{LL} and σ_{LT} are equilibrating stresses in elastic spring, and Kelvin element for longitudinal and transverse strains, respectively. σ_{TT} and σ_{TL} are equilibrating stresses in elastic spring, and Kelvin element for transverse and longitudinal strains, respectively

finite element software, where the corresponding constitutive equations are as follows

$$\begin{bmatrix} \sigma_{\mathrm{L}} \\ \sigma_{\mathrm{T}} \\ \tau \end{bmatrix} = \begin{bmatrix} Q^0_{\mathrm{LL}} & Q^0_{\mathrm{LT}} & 0 \\ Q^0_{\mathrm{TL}} & Q^0_{\mathrm{TT}} & 0 \\ 0 & 0 & Q^0_{\mathrm{LTs}} \end{bmatrix} \begin{bmatrix} \varepsilon^0_{\mathrm{L}} \\ \varepsilon^0_{\mathrm{T}} \\ \gamma^0 \end{bmatrix}, \tag{3}$$

$$\begin{bmatrix} \sigma_{\mathrm{L}} \\ \sigma_{\mathrm{T}} \\ \tau \end{bmatrix} = \begin{bmatrix} \eta^2_{\mathrm{LL}} & \eta^2_{\mathrm{LT}} & 0 \\ \eta^2_{\mathrm{TL}} & \eta^2_{\mathrm{TT}} & 0 \\ 0 & 0 & \eta^2_{\mathrm{LTs}} \end{bmatrix} \begin{bmatrix} \dot{\varepsilon}^2_{\mathrm{L}} \\ \dot{\varepsilon}^2_{\mathrm{T}} \\ \dot{\gamma}^2 \end{bmatrix}, \tag{4}$$

$$\begin{bmatrix} \sigma_{\mathrm{L}} \\ \sigma_{\mathrm{T}} \\ \tau \end{bmatrix} = \begin{bmatrix} Q^i_{\mathrm{LL}} & Q^i_{\mathrm{LT}} & 0 \\ Q^i_{\mathrm{TL}} & Q^i_{\mathrm{TT}} & 0 \\ 0 & 0 & Q^i_{\mathrm{LTs}} \end{bmatrix} \begin{bmatrix} \varepsilon^i_{\mathrm{L}} \\ \varepsilon^i_{\mathrm{T}} \\ \gamma^i \end{bmatrix} + \begin{bmatrix} \eta^i_{\mathrm{LL}} & \eta^i_{\mathrm{LT}} & 0 \\ \eta^i_{\mathrm{TL}} & \eta^i_{\mathrm{TT}} & 0 \\ 0 & 0 & \eta^i_{\mathrm{LTs}} \end{bmatrix} \begin{bmatrix} \dot{\varepsilon}^i_{\mathrm{L}} \\ \dot{\varepsilon}^i_{\mathrm{T}} \\ \dot{\gamma}^i \end{bmatrix} \tag{5}$$

for $i = 1,$ or 1 and 2

where (.) d τ the shear stress and the index i is not associated with a summation. The elastic material parameters, i.e., components of the elastic stiffness matrix in Eq. (3) are determined from relations of elastic moduli and Poisson's ratios for orthotropic material. The viscoelastic response in each model is prescribed in a form from partial differential Eqs. (4) and (5). For clarity, all models constitute Eq. (3); additionally, the K model (Fig. 2) constitutes Eq. (5) for $i = 1$, the KD model Eqs. (4) and (5) for $i = 1$, and the KK model Eq. (5) for $i = 1$ and 2. The formulation of the K model is identical to the one proposed by Frandsen (2007). The KD model has already been applied to the results of Taniguchi and Ando (2010) by Kawahara et al. (2015). Formulation of the model was based on an analytic approach, considering only the loading phase. With that approach, numerical values of material parameters in Eqs. (3)–(5) were impossible to find. To the authors' knowledge, the K and KK models are calibrated against experimental data in the current study for the first time.

In Eqs. (3)–(5), shear stress–strain state in terms of rheological elements is also included. Shear behavior of the material is not coupled to the longitudinal or transverse response of the material. Therefore, the material's viscoelastic response in shear can be formulated separately with the use of basic viscoelastic elements in one dimension. The shear models are directly associated with schematic illustrations of Fig. 1. The set of Eqs. (3)–(5) present a complete mathematical description of the two-dimensional orthotropic behavior of wood. The solution can be obtained elegantly by means of the numerical finite element software.

In general, the more complex the rheological model, the better the fit to experimental data, and the higher the number of unknown material parameters (Q, η). For viscoelastic compliance matrix to be symmetric, the symmetry of 3×3 matrices in Eqs. (4) and (5) is required. Therefore, the simplest two-dimensional K model includes six material parameters. The KD and KK models require 9 and 12 material parameters, respectively. The values of the material parameters dictate the magnitude of the equilibrating stresses that induce strains in longitudinal and

transverse directions [Eq. (2)] when the material is stressed in one or another direction.

The three proposed models are evaluated on four different sets of experimental data from tension tests (Schniewind and Barrett 1972; Hayashi et al. 1993; Taniguchi and Ando 2010; Ożyhar et al. 2013) and one set of data obtained in shear tests by Schniewind and Barrett (1972). Input parameters for the models, such as elastic moduli, Poisson's ratios, shear modulus, and geometry data, as well as experimental viscoelastic creep strains in longitudinal and transverse directions used for the determination of the material parameters, are taken from the tabulated and pictorial data from each article. Unfortunately, no original experimental data have been available to the authors. Schniewind and Barrett (1972) reported an unexpected finding or possibly an error of negative transverse creep that indicates positive creep strain in transverse direction under tensile load in longitudinal direction. Similarly, Ożyhar et al. (2013) noticed a decreasing transverse strain for the specimen under compression in longitudinal direction. Since it is not clear whether the finding is physically feasible in wood material, and the tension tests of the other researchers (Hayashi et al. 1993; Taniguchi and Ando 2010; Ożyhar et al. 2013) did not show such a behavior, the present paper accounts for the positive relative creep in transverse direction and consequently the negative total transverse strain in longitudinal tensile loading. The unknown material parameters of each model are determined by least-squares fitting procedure of numerically predicted against experimentally obtained total strains development in longitudinal and transverse directions simultaneously. The calibration of the models is only executed in loading phase of the tensile and shear data. The material parameters in the three models are determined for four different wood species listed in Table 1, where also abbreviations related to the sets of experimental data used in this manuscript are given. Since Schniewind and Barrett (1972), Taniguchi and Ando (2010), and Hayashi et al. (1993) measured the strains with strain gauges glued directly on the specimen surface, it is suspected that the sample experienced not only the viscoelastic creep but also a portion of mechano-sorptive creep when tested. Change of electrical resistance in the strain gauge produces heat that increases temperature locally on a specimen which causes moisture changes and consequently the wood specimen to experience mechano-sorptive creep. The problem could be significant considering that the magnitude of mechano-sorptive strains might be dominating. However, the possible mechano-sorptive strains are not specifically addressed in this paper and are assumed to be small enough to be neglected.

In the present paper, the complexity of the models according to the number of material parameters needed is tried to be evaluated against the accuracy of

Table 1 Researchers and wood species tested in relation to abbreviations used in this manuscript

Experimental data	Wood species	Abbreviations
Schniewind and Barrett (1972)	Douglas fir	SB
Hayashi et al. (1993)	Norway spruce	HA
Taniguchi and Ando (2010)	Japanese cypress	TA
Ożyhar et al. (2013)	European beech	OZ

numerically obtained strain development due to tensile and shear loading in comparison to available experimental data. The accuracy of a particular model is evaluated by an average of absolute value of relative errors (RE) of predicted strains at observed times, and by a method presented in Annex D in EN (1990). The evaluation parameters are determined for the strain development predicted by each model in the longitudinal and the transverse directions separately, as well as for both directions together, L + T. In total, the comparison method analyzes 42 different cases that cover the three viscoelastic constitutive models calibrated to five sets of experimental data in loading phase, including shear and constant tension in longitudinal and transverse direction separately and combined. The method presented in Annex D in EN (1990) includes an estimation of the mean value correction factor b that is the "least-squares" best fit to the slope, and the coefficient of variation, V_{δ}, of the lognormally distributed error terms. In regression analysis, the term b is recognized as the slope of the regression line that tells the amount by which the experimental variable increases or decreases, on average, when the numerical variable increases by one. Practically, that means if the value of b is larger than one, the numerically predicted values are smaller than experimental values of creep strains on average. In that case, the particular constitutive model underestimates the experimental data on average. On the contrary, when the b value is smaller than one, the constitutive model overestimates the creep strains on average. Coefficient of variation, V_{δ}, is a measure of an average scatter of the numerical value from the experimental value at each point compared. Hence, the smaller the coefficient of variation, the better the constitutive model predicts the experimentally observed values of creep strains.

Results and discussion

Figures 3, 4, 5, 6, and 7 show predicted (lines) and actual, experimentally measured (diamond markers, *abbrev.* exp) two-dimensional viscoelastic response of four different wood species. The abbreviations for each set of data (Table 1) are used in combination with the label of the type of the creep model, explained earlier (K, KD, and KK), which ends up in 12 combinations in tension and three in shear. Reason for making those combinations of labels is related to different values of material parameters determined by the fitting procedure of particular creep model to a particular set of experimental data. The calculated values of the material parameters (given in Tables A1 and A2 in Online Resource) characterize each type of analyzed creep model fitted to specific experimental data. The examined wood specimens are loaded under constant tension in longitudinal (Figs. 3b, c, 4, 5, 6) and transverse directions (Fig. 3a). Taniguchi and Ando (2010) also presented strain response after unloading for a period of extra 24 h (Fig. 5). Experimental data of pure viscoelastic shear behavior of Douglas fir are extracted from Schniewind and Barrett (1972). Time interval of monitored viscoelastic creep response in loading phase differs among the experimental data, from 16.67 h (SB exp), 100 h (HA exp) to 24 h (TA exp and OZ exp). The longitudinal strain, εL, and the transverse strain, εT, that is the strain in radial orthotropic direction of wood, are related to the data HA, TA, and

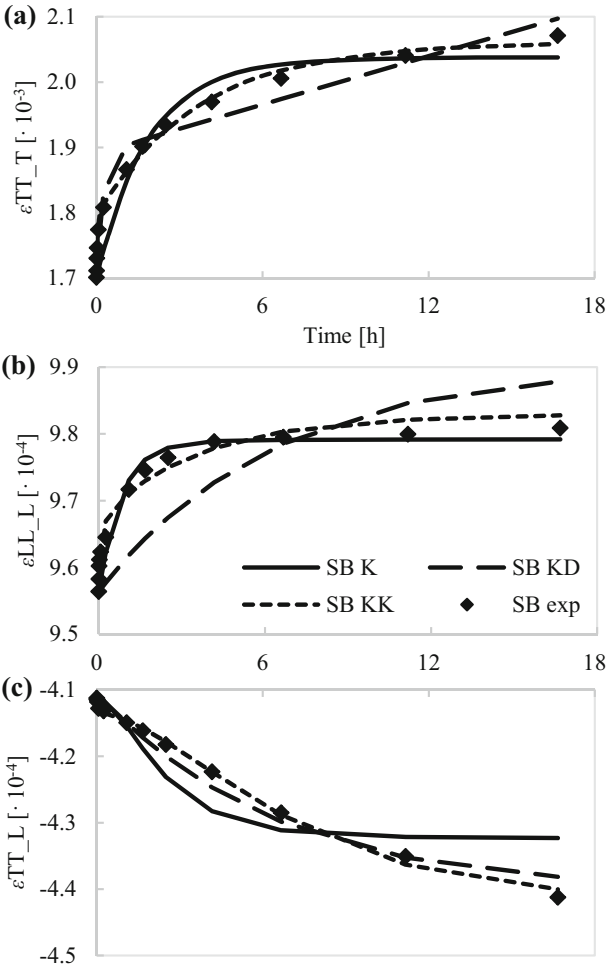

Fig. 3 Viscoelastic creep in **a** transverse direction when tensile load is applied in transverse direction, **b** longitudinal and **c** transverse direction when wood specimen is exposed to constant tensile load in longitudinal direction. Experimental data (exp) for Douglas fir wood species is extracted from Schniewind and Barrett (1972) (SB), and predicted with the three different coupled constitutive models for orthotropic material (K, KD, and KK)

OZ. In the data related to SB, the longitudinal strain is denoted by εLL_L and the transverse, that is the strain in tangential orthotropic direction of wood, by εTT_L, when the specimen is loaded in longitudinal direction. When the specimen is loaded in the transverse direction, that is the tangential direction, the transverse strain is denoted by εTT_T. No data of longitudinal strain are available for the latter loading mode. Total shear strain measured in tangential–longitudinal plane is denoted by γ in Fig. 7. The predicted curves of viscoelastic strains in longitudinal and transverse directions, and in shear, present the best fit of particular creep model to the experimental data in loading phase.

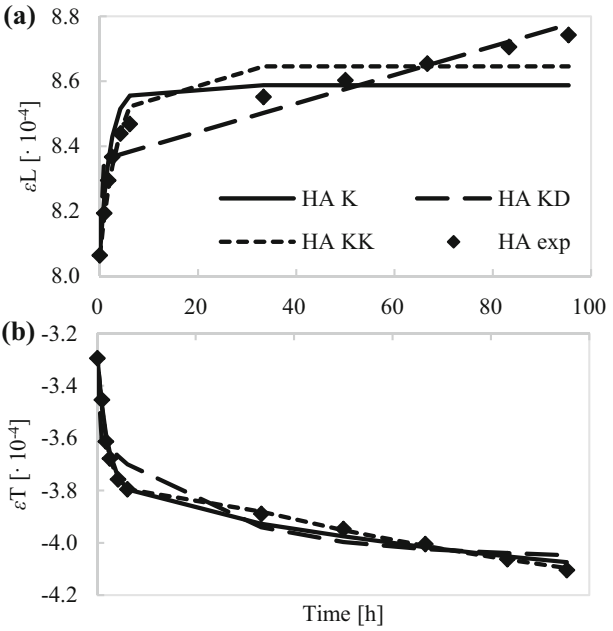

Fig. 4 Viscoelastic creep in **a** longitudinal and **b** transverse direction of Norway spruce exposed to constant tensile load in longitudinal direction. Experimental data (exp) is extracted from Hayashi et al. (1993) (HA), and predicted with the three different coupled constitutive models for orthotropic material (K, KD, and KK)

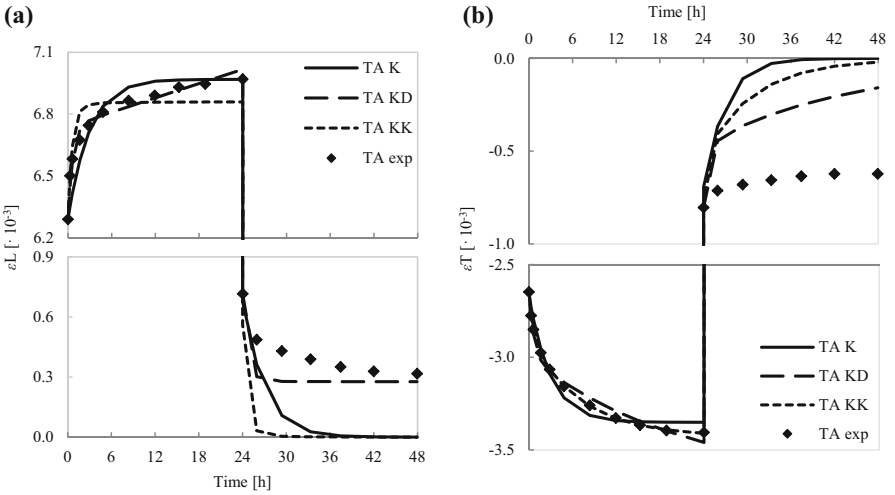

Fig. 5 Viscoelastic creep in **a** longitudinal and **b** transverse direction of Japanese cypress exposed to constant tensile load in longitudinal direction followed by unloading phase. Experimental data (exp) are extracted from Taniguchi and Ando (2010) (TA), and predicted with the three different coupled constitutive models for orthotropic material (K, KD, and KK)

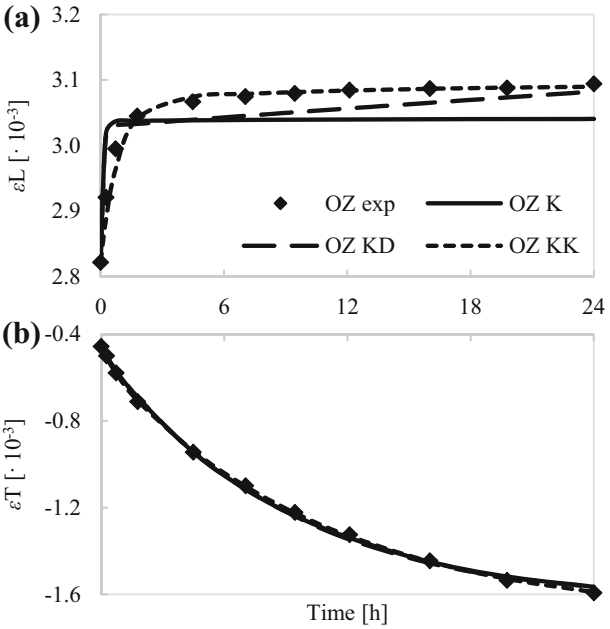

Fig. 6 Viscoelastic creep in **a** longitudinal and **b** transverse direction of European beech wood exposed to constant tensile load in longitudinal direction. Experimental data (exp) is extracted from Ożyhar et al. (2013) (OZ), and predicted with the three different coupled constitutive models for orthotropic material (K, KD, and KK)

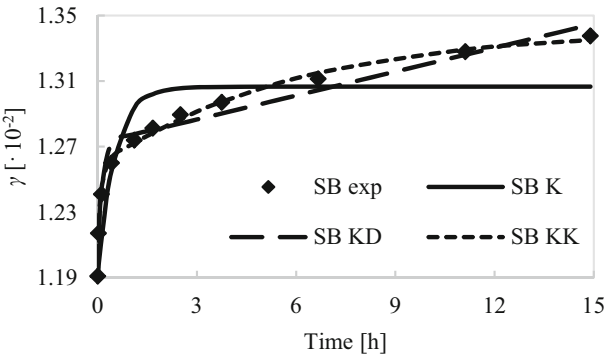

Fig. 7 Long-term behavior of viscoelastic shear strain of Douglas fir. Experimental data (exp) is extracted from Schniewind and Barrett (1972) (SB), and predicted with the three different coupled constitutive models for orthotropic material (K, KD, and KK)

According to the parameter b (Table 2), all three constitutive models on average underestimate the experimental data SB exp in the longitudinal and transverse direction, except the K model which on average overestimates the transverse strain, εTT_L, in SB K case where the tensile load is applied in longitudinal direction. The coefficient of variation, V_δ, indicates that the case SB KK gives the closest fit of

Table 2 Comparison of the three coupled two-dimensional models (K, KD, and KK) on predicted viscoelastic strains in longitudinal and transverse direction separately and together against experimentally obtained data from Schniewind and Barrett (1972)

Case	SB K	SB KD	SB KK
b			
LL_L + TT_L + TT_T	1.0011	1.0031	1.0003
LL_L	1.0011	1.0037	1.0004
TT_L	0.9999	1.0001	1.0001
TT_T	1.0075	1.0024	1.0002
V_δ (%)			
LL_L + TT_L + TT_T	1.12	0.77	0.25
LL_L	0.21	0.55	0.18
TT_L	0.87	0.34	0.13
TT_T	1.64	1.18	0.39
RE (%)			
LL_L + TT_L + TT_T	0.72	0.61	0.19
LL_L	0.19	0.56	0.16
TT_L	0.59	0.25	0.08
TT_T	1.37	1.03	0.32

The comparison includes cases where the numerically predicted strains are compared against experimental strains in longitudinal (LL_L) and transverse directions (TT_L) when loaded in longitudinal direction, and transverse strains (TT_T) when loaded in transverse direction. RE denotes the average of absolute value of relative error, b the correction factor, and V_δ the coefficient of variation

measured strains in longitudinal and transverse directions separately and together, followed by the cases SB KD, and SB K. Exception is noticed in the longitudinal direction, where SB K gives better fit of εLL_L than SB KD. The case HA KK gives the best fit of experimental results HA exp in all strain directions separately and together (Table 3). According to the values of V_δ, the case HA KD fits the longitudinal strain, εL, better than the case HA K. The opposite is noticed by the strain in transverse direction, εT, and when the evaluation method is applied to the predicted strains in both directions together. The K model on average underestimates the experimental results TA exp in the case TA K in all directions considered separately and together. The comparison of the magnitude of V_δ in TA cases shows that the KK model is the best in predicting the transverse strain alone, while the longitudinal strain and strains in both directions together are better predicted by the KD model. When comparing the predicted and the experimental data OZ exp (Table 3), it can be seen that the KK model gives the best fit in longitudinal, transverse, and both directions together.

Magnitudes of the predicted and the experimental strains at final time of loading phase together with the strain growth trend are interesting to observe, in particular, in cases, when the predicted strain rates are significantly smaller than the experimentally measured. This type of underestimation of prediction will be severe when extrapolated. The strain predictions of K models is such a case, where the

Table 3 Comparison of the three coupled two-dimensional models (K, KD, and KK) on predicted viscoelastic strains in longitudinal and transverse direction separately and together due to constant tensile loading in longitudinal direction against experimentally obtained data from Hayashi et al. (1993) (HA), Taniguchi and Ando (2010) (TA), and Ożyhar et al. (2013) (OZ)

Case	HA K	HA KD	HA KK	TA K	TA KD	TA KK	OZ K	OZ KD	OZ KK
b									
L + T	0.9999	0.9992	1.0004	1.0027	1.0000	0.9996	1.0046	1.0012	1.0015
L	0.9999	0.9991	1.0004	1.0028	1.0000	0.9995	1.0050	1.0014	1.0018
T	1.0003	0.9999	1.0001	1.0024	0.9997	1.0000	1.0014	0.9999	0.9999
V_δ (%)									
L + T	0.78	1.47	0.48	1.27	0.71	0.80	1.47	1.39	0.50
L	0.96	0.84	0.62	1.24	0.44	1.14	1.56	1.24	0.47
T	0.60	1.96	0.31	1.36	0.93	0.18	1.43	1.59	0.52
RE (%)									
L + T	0.63	1.05	0.34	1.03	0.54	0.50	1.24	1.07	0.34
L	0.77	0.60	0.46	0.91	0.35	0.88	1.33	0.91	0.27
T	0.49	1.50	0.22	1.15	0.73	0.12	1.15	1.23	0.41

RE denotes the average of absolute value of relative error, *b* the correction factor, and V_δ the coefficient of variation

strain rate at the end of predicted results in loading phase is negligible, while the strain rate of experimental results is still evident. Besides the observed variations in strains growth trend, the highest RE at final time of loading phase is noticed in the K model prediction of the transverse strain εTT_L (Fig. 3c), RE ($t = 16.67$ h) = 2.0% in the case SB K. The KD model overestimates the strains at final observed time of loading phase in the cases of the longitudinal strains εL (HA KD, Fig. 4a and TA KD, Fig. 5a), the transverse strain εT (TA KD, Fig. 5b), and the transverse εTT_T and the longitudinal strain εLL_L (SB KD, Fig. 3a, b, respectively). The most remarkable overestimation of the KD model is noticed in the case TA KD ($t = 24$ h) and results in RE = 1.7% when predicting the strain in the transverse direction εT (Fig. 5b). In all other cases, KD model underestimates the values of strains at final time. The largest underestimation is noticed in the prediction of the transverse strain εT in the case OZ KD (Fig. 6b), which results in RE = 1.7% at $t = 24$ h. The KK model tends to slightly underestimate the strains at final observed times. The maximum underestimation is noticed in the predictions of the longitudinal strain εL at $t = 24$ h in the case TA KK (Fig. 5a) and amounts to RE = 1.6%. It can be concluded that the K and KK models have a tendency to underestimate the strains at final time of loading phase, which could potentially be unsafe, while the KD model can both under and overestimate the strains at final observed time of loading phase of wood specimen under tension.

The evaluation parameters for the three constitutive models for viscoelastic creep of wood in shear (Table 4) reveal that all three models on average underestimate the experimental data SB exp (Fig. 7). The KK model gives the best fit, since the value of $V_\delta = 0.21\%$. The worst fit is obtained by the K model, where the viscoelastic

shear creep strain reaches its limit value $\gamma = 1.31 \times 10^{-2}$ at $t = 6.67$ h. In that case, the relative error of predicted shear strain at final time equals to RE = 2.3%.

Generally, the results in Figs. 3, 4, 5, 6, and 7 are presented on a large scale that makes the behavior of the constitutive models' predictions quite visible and could on some occasions give false impression on the accuracy of the results. Though there are some visible differences in models predictions, RE of predicted strains in all cases is less or equal to 1.50%. The error can be considered as very small taking into account the reasonable likelihood that some amount of error has already been introduced by measuring and plotting the results, and finally by extracting the data from pictorial in the papers, since no original measurements are available to the authors.

The experimental data by Taniguchi and Ando (2010) include not only the viscoelastic strain response of a wood specimen under constant tensile load in longitudinal direction but also the response after unloading (Fig. 5). The unloading and the following creep return are predicted by the three constitutive models where the material parameters determined by fitting procedure of the loading phase are used (Table A.1 in Online Resource). It can be seen (Fig. 5) that the models predict the strain recovery after unloading relatively poor. The elastic return is predicted perfectly by all models, followed by complete strain recovery by the K and KK models in both directions, since they cannot retain non-recoverable strain. On the other hand, the KD model is able to simultaneously predict unrecoverable part of the total strain in longitudinal and transverse direction. It is obvious that after 24 h of recovery, the longitudinal strain prediction is much better than the transverse strain prediction of the KD model.

The predicted values of the material parameters applicable to all three models are given in Tables A1 and A2 in Online Resource and present another significant outcome of the performed analysis. Due to requirements of the formulation of the models, the material parameters are positive values of the magnitude up to 10^{17}. They are given with precision of 15 digits, since it is observed that a relatively small variation (on a 14th decimal place) of some parameters can cause a noticeable change in the strain response. Sensitivity of the material parameters is not studied in the present paper; therefore, it is decided to show all the digits of the material parameters as they are derived in the analysis.

Table 4 Comparison of the three different constitutive models for shear (K, KD, and KK) on numerically predicted shear strains against experimentally obtained data from Schniewind and Barrett (1972)

Shear	SB K	SB KD	SB KK
b	1.0030	1.0004	1.0001
V_δ (%)	1.49	0.48	0.21
RE (%)	1.25	0.38	0.18

RE denotes the average of absolute value of relative errors, b the correction factor, and V_δ the coefficient of variation

Conclusion

The paper shows applicability and formulation of the three coupled two-dimensional creep models for orthotropic material based on the theory presented by Frandsen (2007). Complexity of the models differs and is connected to the number of material parameters needed in the particular formulation. The models are calibrated against the experimental data and the material parameters are determined for four wood species when loaded in constant tension, namely Douglas fir, spruce, Japanese cypress, and European beech. Additionally, the material parameters for Douglas fir exposed to constant shear load are given. Therefore, this paper delivers formulations of the three completely coupled two-dimensional constitutive orthotropic models together with numerical values of the material parameters for Douglas fir wood species. According to the comparison method for experimental and numerical data, it can be concluded that all the models are capable to predict viscoelastic creep of wood for the time periods studied. Nevertheless, the comparison method shows that the most complex model (KK) also gives the best predictions of strains in the majority of analyzed cases; when accounting for relatively small errors already, the simplest model (K) can be considered as useful enough for describing viscoelastic creep of wood in two dimensions. That may prove as important when additional phenomena connected to the long-term behavior of wood, i.e., mechano-sorptive creep, are included in the model, and at the same time, the number of unknown material parameters is desired to be kept as few as possible. Application of the constitutive models in the finite element software and simultaneous fitting procedure to the available experimental data allows obtaining numerical values of the material parameters for different wood species.

The presented extensive analysis of the three coupled two-dimensional models of viscoelastic creep of wood initiated some ideas for future work. To get more detailed insight into models' functioning and find the degree of influence of a particular material parameter on final output in different time periods, a sensitivity analysis is needed. It could be helpful in finding potential relations between the parameters and reducing the number of digits required as well. Studying the ability of the models to predict mechano-sorptive creep, and their improvement and validation for cyclic loading might also be interesting. A great challenge would present an upgrade of the models' formulations to three dimensions that are able to describe a complete long-term behavior of timber elements under changing environmental conditions. Certainly, the presented rheological constitutive models have a potential to complement or reduce experimental work needed for finding accurate and sufficient values of the material parameters of various wood species that will allow optimal design of timber structures.

Acknowledgements The financial support by Gunnar Ivarson's Foundation (Gunnar Ivarsons Stiftelse för Hållbart Samhällsbyggande, GIS) made this work possible.

References

Ando K, Mizutani M, Taniguchi Y, Yamamoto H (2013) Time dependence of Poisson's effect in wood III: asymmetry of three-dimensional viscoelastic compliance matrix of Japanese cypress. J Wood Sci 59:290–298

Bonfield PW, Mundy J, Robson DJ, Dinwoodie JM (1996) The modelling of time-dependant deformation in wood using chemical kinetics. Wood Sci Technol 30:105–115

Caulfield DF (1985) A chemical kinetics approach to the duration-of-load problem in wood. Wood Fiber Sci 17:504–521

Colmars J, Dubois F, Gril J (2014) One-dimensional discrete formulation of a hygrolock model for wood hygromechanics. Mech Time Depend Mater 18:309–328

Dubois F, Randriambololona H, Petit C (2005) Creep in wood under variable climate conditions: numerical modeling and experimental validation. Mech Time Depend Mater 9:173–202

Dubois F, Husson JM, Sauvat N, Manfoumbi N (2012) Modeling of the viscoelastic mechano-sorptive behavior in wood. Mech Time Depend Mater 16:439–460

EN 1990 (2002) Annex D, Eurocode—Basis of structural design, Brussels

Engelund ET, Svensson S (2011) Modelling time-dependent mechanical behaviour of softwood using deformation kinetics. Holzforschung 65:231–237

Flügge W (1967) Viscoelasticity. Blaisdell Publishing Company, University of Michigan, Waltham

Fortino S, Mirianon F, Toratti T (2009) A 3D moisture-stress FEM analysis for time dependent problems in timber structures. Mech Time Depend Mater 13:333–356

Frandsen HL (2007) Selected constitutive models for simulating the hygromechanical response of wood. Ph.D. Thesis, Aalborg University, Denmark, pp 87–104

Hanhijärvi A (1995) Deformation kinetics based rheological model for the time-dependent and moisture induced deformation of wood. Wood Sci Technol 29:191–199

Hanhijärvi A, Hunt D (1998) Experimental indication of interaction between viscoelastic and mechano-sorptive creep. Wood Sci Technol 32:57–70

Hassani MM, Wittel FK, Hering S, Herrman HJ (2015) Rheological model for wood. Comput Methods Appl Mech Eng 283:1032–1060

Hayashi K, Felix B, Le Govic C (1993) Wood viscoelastic compliance determination with special attention to measurement problems. Mater Struct 26:370–376

Hunt DG, Gril J (1996) Evidence of physical ageing phenomenon in wood. J Mater Sci Lett 15:80–82

Jiang J, Valentine BE, Lu J, Niemz P (2016) Time dependence of the orthotropic compression Young's moduli and Poisson's ratios of Chinese fir wood. Holzforschung 70:1093–1101

Kawahara K, Ando K, Taniguchi Y (2015) Time dependence of Poisson's effect in wood IV: influence of grain angle. J Wood Sci 61:372–383

Ormarsson S (1999) Numerical analysis of moisture-related distortions in sawn timber. Ph.D. thesis, Chalmers University of Technology, Göteborg

Ożyhar T, Hering S, Niemz P (2013) Viscoelastic characterization of wood: time dependence of the orthotropic compliance in tension and compression. J Rheol 57:699–717

Reichel S, Kaliske M (2015a) Hygro-mechanically coupled modelling of creep in wooden structures, part I: mechanics. Int J Solids Struct 77:28–44

Reichel S, Kaliske M (2015b) Hygro-mechanically coupled modelling of creep in wooden structures, part II: influence of moisture content. Int J Solids Struct 77:45–64

Schniewind AP, Barrett JD (1972) Wood as a linear viscoelastic material. Wood Sci Technol 6:43–57

Taniguchi Y, Ando K (2010) Time dependence of Poisson's effect in wood I: the lateral strain behavior. J Wood Sci 56:100–106

Toratti T, Svensson S (2000) Mechano-sorptive experiments perpendicular to grain under tensile and compressive loads. Wood Sci Technol 34:317–326